Matrix approach for light scattering by bianisotropic cylindrical particles

2007 J. Phys.: Condens. Matter 19 086213

(http://iopscience.iop.org/0953-8984/19/8/086213)

IOP PUBLISHING JOURNAL OF PHYSICS: CONDENSED MATTER

J. Phys.: Condens. Matter **19** (2007) 086213 (11pp) doi:10.1088/0953-8984/19/8/086213

Matrix approach for light scattering by bianisotropic cylindrical particles

A V Novitsky

Department of Theoretical Physics, Belarusian State University, Nezavisimosti Avenue 4, 220050 Minsk, Belarus

E-mail: andrey.novitsky@tut.by

Received 11 September 2006, in final form 29 December 2006
Published 9 February 2007
Online at stacks.iop.org/JPhysCM/19/086213

Abstract
Using a matrix (operator) method, the problem of scattering of arbitrary electromagnetic waves by multilayer bianisotropic cylinders is solved. The scattering of a Gaussian beam is considered as an example.

(Some figures in this article are in colour only in the electronic version)

1. Introduction

Scattering is one of the fundamental problems of theoretical and experimental physics [1, 2]. There are various types of scattering, such as electromagnetic wave scattering (by dielectric or metal particles, by spherical or cylindrical particles, etc) and particle scattering by a potential (classical or quantum scattering of spin or spinless particles). The theory of particle scattering is widely used in quantum field theories and nuclear physics. In this paper we deal only with the scattering of electromagnetic fields by circular cylinders.

Cylindrically symmetric objects have been studied for a long time. Nowadays, there are many applications of cylinders guiding electromagnetic waves. Dielectric or metal circular fibres can be used not only for optical communications [3] but also for designing sensors [4]. New types of materials (e.g. bianisotropic materials) are promising for the creation of devices with peculiar properties. Fibre sensors can be applied to detect magnetic fields and electric currents (on the basis of the magnetostrictive principle) [5], twist and pressure (e.g. in highly birefringent bow-tie fibres [6]), etc. In [7] a method for fibre sensing based on an analysis of the forward-scattering intensity pattern is described. That approach is less sophisticated and less costly than the methods used previously.

Some other applications of scattering are presented below. First, the scattering of a wave by chiral cylinders [8–10], which can emulate biological objects, is studied. Second, attention is focused on scattering by a cylinder fabricated from a left-handed material [11–13]. Left-handed materials (negative-refractive media, metamaterials) simultaneously possess negative dielectric and magnetic permittivities [14, 15]. Therefore, electromagnetic waves propagate in a sufficiently different way compared with traditional media and new scattering properties are foreseen. One more application is connected with phase-Doppler anemometry. Phase-Doppler anemometry is an optical technique for simultaneous measurement of the velocity and the size of spherical particles in flows. In [16, 17] an attempt to generalize that technique to the characterization of cylindrical particles was made.

The study of the diffraction of electromagnetic waves in complex media is a great challenge. Theoretical research in this field was made, for example, in [18–20]. The authors investigated the scattering of obliquely incident waves by a perfectly conducting strip. The strip can be situated both in an unbounded bianisotropic (biisotropic, gyrotropic) medium or in a bianisotropic cylinder. To solve such a complicated problem, the authors derived systems of singular integral–integrodifferential equations having the induced surface current densities as the unknowns. The technique offered is very effective for calculation of the cross-sections of ordinary and extraordinary electromagnetic waves. In [21] the electromagnetic scattering from chiral circular cylinders with different locations and radii was investigated using an iterative scattering procedure. The cylinders can be made of anisotropic chiral material with a uniform or non-uniform chiral admittance distribution, a homogeneous isotropic dielectric material, a perfectly conducting material or a combination of all of these. In [22] a modelling technique based on the principle of the equivolumetric model was applied to describe multiple scattering from bianisotropic cylinders. Another problem to investigate is electromagnetic scattering by a multilayer gyrotropic bianisotropic circular cylinder. The authors of [23] derived coupled wave equations for longitudinal field components and applied the eigenfunction expansion method. Linear algebraic equations were solved with and without the centre being a perfect electric conducting cylinder. Some results for the scattering by arrays of cylinders can be obtained in the eikonal approximation [24].

Our investigation allows us to advance in each of the directions mentioned above because we develop a new matrix method to describe the scattering of arbitrary electromagnetic fields by multilayer bianisotropic cylinders. In section 2 the basic concepts of our method are presented. Our matrix (operator) techniques were verified earlier for the cases of optical fibres [25] and beams [26], as well as for electromagnetic scattering by spherical particles [27]. Section 3 is devoted to scattering by cylinders. Section 4 contains a study of the scattering of a Gaussian beam by a bianisotropic cylinder with isotropic cladding.

2. Vector cylindrical solutions of Maxwell's equations in bianisotropic media

We use the well-known definition of bianisotropic media as general media with four tensor linear characteristics in constitutive equations

$$\boldsymbol{D} = \varepsilon \boldsymbol{E} + \alpha \boldsymbol{H} \qquad \boldsymbol{B} = \kappa \boldsymbol{E} + \mu \boldsymbol{H} \tag{1}$$

where $\boldsymbol{H}$, $\boldsymbol{E}$, $\boldsymbol{B}$ and $\boldsymbol{D}$ are strengths and inductions of magnetic and electric fields, ε and μ are dielectric permittivity and magnetic permeability tensors, respectively, and α and κ are gyration tensors. We consider only cylindrically symmetric tensors $\xi = \{\varepsilon, \mu, \alpha, \kappa\}$

$$\xi = \xi_1 I_z + \xi_2 \boldsymbol{e}_z \otimes \boldsymbol{e}_z + \mathrm{i}\chi_\xi \boldsymbol{e}_z^\times \tag{2}$$

where (r, φ, z) are cylindrical coordinates, $\boldsymbol{e}_1 = \boldsymbol{e}_r(\varphi)$, $\boldsymbol{e}_2 = \boldsymbol{e}_\varphi(\varphi)$, $\boldsymbol{e}_3 = \boldsymbol{e}_z$ are the basis vectors in cylindrical coordinates, $\boldsymbol{e}_i \otimes \boldsymbol{e}_j$ is the dyad; $\boldsymbol{e}_z^\times$ is the tensor dual to the vector $\boldsymbol{e}_z$ [25–28] and $I_z = 1 - \boldsymbol{e}_z \otimes \boldsymbol{e}_z$ is the projection operator onto the plane perpendicular to vector $\boldsymbol{e}_z$. Scalar coefficients ξ_1, ξ_2 and χ_ξ are constant values. The eigenwaves in the medium (2) can be called cylindrical electromagnetic waves. They can be described as follows

$$\begin{pmatrix} \boldsymbol{H}(\boldsymbol{r}, t) \\ \boldsymbol{E}(\boldsymbol{r}, t) \end{pmatrix} = \mathrm{e}^{\mathrm{i}\beta z + \mathrm{i}\nu\varphi - \mathrm{i}\omega t} \begin{pmatrix} \boldsymbol{H}(r) \\ \boldsymbol{E}(r) \end{pmatrix} \tag{3}$$

where β is the longitudinal wavenumber, ω is the wave frequency and ν is the azimuthal number taking integer values. As a result, one can reduce the Maxwell equations to a system of ordinary differential equations of the first order [25] for tangential field components

$$\frac{\mathrm{d}\boldsymbol{W}(r)}{\mathrm{d}r} = \mathrm{i}kM(r)\boldsymbol{W}(r) \tag{4}$$

where

$$\begin{aligned}
&M = \begin{pmatrix} A & B \\ C & D \end{pmatrix} \qquad \boldsymbol{W} = \begin{pmatrix} \boldsymbol{H}_\mathrm{t} \\ \boldsymbol{E}_\mathrm{t} \end{pmatrix} \\
&A = \frac{\mathrm{i}}{kr}\boldsymbol{e}_\varphi \otimes \boldsymbol{e}_\varphi + \boldsymbol{e}_r^\times \alpha I_r + \boldsymbol{e}_r^\times \varepsilon \boldsymbol{e}_r \otimes \boldsymbol{v}_3 + \boldsymbol{e}_r^\times (\boldsymbol{u} + \alpha \boldsymbol{e}_r) \otimes \boldsymbol{v}_1 \\
&B = \boldsymbol{e}_r^\times \varepsilon I_r + \boldsymbol{e}_r^\times \varepsilon \boldsymbol{e}_r \otimes \boldsymbol{v}_4 + \boldsymbol{e}_r^\times (\boldsymbol{u} + \alpha \boldsymbol{e}_r) \otimes \boldsymbol{v}_2 \\
&C = -\boldsymbol{e}_r^\times \mu I_r - \boldsymbol{e}_r^\times \mu \boldsymbol{e}_r \otimes \boldsymbol{v}_1 + \boldsymbol{e}_r^\times (\boldsymbol{u} - \kappa \boldsymbol{e}_r) \otimes \boldsymbol{v}_3 \\
&D = \frac{\mathrm{i}}{kr}\boldsymbol{e}_\varphi \otimes \boldsymbol{e}_\varphi - \boldsymbol{e}_r^\times \kappa I_r - \boldsymbol{e}_r^\times \mu \boldsymbol{e}_r \otimes \boldsymbol{v}_2 + \boldsymbol{e}_r^\times (\boldsymbol{u} - \kappa \boldsymbol{e}_r) \otimes \boldsymbol{v}_4 \\
&\boldsymbol{v}_1 = \delta_r(\kappa_{rr}\boldsymbol{e}_r \alpha I_r - \varepsilon_{rr}\boldsymbol{e}_r \mu I_r - \kappa_{rr}\boldsymbol{u}) \qquad \boldsymbol{v}_2 = \delta_r(\kappa_{rr}\boldsymbol{e}_r \varepsilon I_r - \varepsilon_{rr}\boldsymbol{e}_r \kappa I_r - \varepsilon_{rr}\boldsymbol{u}) \\
&\boldsymbol{v}_3 = \delta_r(\alpha_{rr}\boldsymbol{e}_r \mu I_r - \mu_{rr}\boldsymbol{e}_r \alpha I_r + \mu_{rr}\boldsymbol{u}) \qquad \boldsymbol{v}_4 = \delta_r(\alpha_{rr}\boldsymbol{e}_r \kappa I_r - \mu_{rr}\boldsymbol{e}_r \varepsilon I_r + \alpha_{rr}\boldsymbol{u}) \\
&\boldsymbol{u} = (\beta/k)\boldsymbol{e}_\varphi - \nu/(kr)\boldsymbol{e}_z \qquad \delta_r = (\varepsilon_{rr}\mu_{rr} - \alpha_{rr}\kappa_{rr})^{-1} \\
&\varepsilon_{rr} = \boldsymbol{e}_r \varepsilon \boldsymbol{e}_r, \qquad \mu_{rr} = \boldsymbol{e}_r \mu \boldsymbol{e}_r \qquad \alpha_{rr} = \boldsymbol{e}_r \alpha \boldsymbol{e}_r \qquad \kappa_{rr} = \boldsymbol{e}_r \kappa \boldsymbol{e}_r.
\end{aligned} \tag{5}$$

Tangential components of strength vectors are situated in the plane (φ, z) and are equal to $\boldsymbol{E}_t = I_r\boldsymbol{E}$ and $\boldsymbol{H}_t = I_r\boldsymbol{H}$, where $I_r = 1 - \boldsymbol{e}_r \otimes \boldsymbol{e}_r$ is the projection operator onto the plane orthogonal to the unit vector $\boldsymbol{e}_r$ and $k = \omega/c$ is the vacuum wavenumber. We should note that the system of differential equations of the first order for planar stratified media was derived earlier in [29].

In a number of papers we obtained some cylindrical solutions for isotropic, biisotropic and bianisotropic media. Here, we briefly demonstrate how to obtain these solutions, based on the paper [25]. Matrix M is the matrix function with respect to the radial coordinate r:

$$M = M^{(0)} + \frac{1}{r}M^{(1)} + \frac{1}{r^2}M^{(2)} \tag{6}$$

where

$$\begin{aligned}
&M^{(0)} = M^{(0)}_{z\varphi}\boldsymbol{e}_z \otimes \boldsymbol{e}_\varphi + M^{(0)}_{\varphi z}\boldsymbol{e}_\varphi \otimes \boldsymbol{e}_z \\
&M^{(1)} = M^{(1)}_{zz}\boldsymbol{e}_z \otimes \boldsymbol{e}_z + M^{(1)}_{\varphi\varphi}\boldsymbol{e}_\varphi \otimes \boldsymbol{e}_\varphi \qquad M^{(2)} = M^{(2)}_{\varphi z}\boldsymbol{e}_\varphi \otimes \boldsymbol{e}_z.
\end{aligned} \tag{7}$$

2×2 matrices $M^{(0)}_{z\varphi}$, $M^{(0)}_{\varphi z}$, $M^{(1)}_{zz}$, $M_{\varphi\varphi}$ and $M^{(2)}_{\varphi z}$ can be determined from (5). They are simple for isotropic media and cumbersome for bianisotropic media. Complicated matrices can be calculated using a computer.

Further, we can find longitudinal field components of the wave propagating in a bianisotropic medium (2) from the differential equation

$$\frac{\mathrm{d}^2}{\mathrm{d}r^2}\begin{pmatrix} H_z \\ E_z \end{pmatrix} + \frac{1}{r}\frac{\mathrm{d}}{\mathrm{d}r}\begin{pmatrix} H_z \\ E_z \end{pmatrix} + \left(Q - \frac{\nu^2}{r^2}\begin{pmatrix} 1 & 0 \\ 0 & 1 \end{pmatrix}\right)\begin{pmatrix} H_z \\ E_z \end{pmatrix} = 0 \tag{8}$$

where $Q = k^2 M^{(0)}_{z\varphi} M^{(0)}_{\varphi z}$ is a two-dimensional matrix. It is obvious that the solutions of equation (8) are Bessel functions of the first $J_{|\nu|}$ and second $Y_{|\nu|}$ kind of order $|\nu|$. Using the spectral decomposition for matrix Q one obtains

$$\begin{pmatrix} H_z \\ E_z \end{pmatrix} = (c_1 J_{|\nu|}(q_1 r) + c_3 Y_{|\nu|}(q_1 r))\vec{w}_1 + (c_2 J_{|\nu|}(q_2 r) + c_4 Y_{|\nu|}(q_2 r))\vec{w}_2 \tag{9}$$

where q_1^2, q_2^2 are the eigenvalues of Q and $\vec{w}_1$, $\vec{w}_2$ are its eigenvectors. Introducing two vectors $\boldsymbol{c}_1$ and $\boldsymbol{c}_2$ with constant components c_i, $i = 1, 2, 3, 4$ we can write the tangential field components

$$\boldsymbol{W} = \begin{pmatrix} \eta_1(r)\boldsymbol{c}_1 \\ \zeta_1(r)\boldsymbol{c}_1 \end{pmatrix} + \begin{pmatrix} \eta_2(r)\boldsymbol{c}_2 \\ \zeta_2(r)\boldsymbol{c}_2 \end{pmatrix} \tag{10}$$

where planar tensors η_1, ζ_1 equal (planar tensors are defined as $\eta_1 I_r = I_r\eta_1 = \eta_1$)

$$\begin{aligned} \eta_1 = {} & \vec{e}_1\vec{w}_1 J_{|\nu|}(q_1 r)\boldsymbol{e}_z \otimes \boldsymbol{e}_z + \vec{e}_1\hat{Z} J_{|\nu|}(q_1 r)\vec{w}_1\boldsymbol{e}_\varphi \otimes \boldsymbol{e}_z \\ & + \vec{e}_1\vec{w}_2 J_{|\nu|}(q_2 r)\boldsymbol{e}_z \otimes \boldsymbol{e}_\varphi + \vec{e}_1\hat{Z} J_{|\nu|}(q_2 r)\vec{w}_2\boldsymbol{e}_\varphi \otimes \boldsymbol{e}_\varphi \\ \zeta_1 = {} & \vec{e}_2\vec{w}_1 J_{|\nu|}(q_1 r)\boldsymbol{e}_z \otimes \boldsymbol{e}_z + \vec{e}_2\hat{Z} J_{|\nu|}(q_1 r)\vec{w}_1\boldsymbol{e}_\varphi \otimes \boldsymbol{e}_z \\ & + \vec{e}_2\vec{w}_2 J_{|\nu|}(q_2 r)\boldsymbol{e}_z \otimes \boldsymbol{e}_\varphi + \vec{e}_2\hat{Z} J_{|\nu|}(q_2 r)\vec{w}_2\boldsymbol{e}_\varphi \otimes \boldsymbol{e}_\varphi. \end{aligned} \tag{11}$$

Replacing $J_{|\nu|}$ by $Y_{|\nu|}$ one can get the tensors η_2, ζ_2. In expression (11) we introduce unit two-dimensional vectors $\vec{e}_1 = (1\ 0)^{\mathrm{T}}$, $\vec{e}_2 = (0\ 1)^{\mathrm{T}}$ and matrix differential operator $\hat{Z}$ is equal to

$$\hat{Z} = M_{z\varphi}^{(0)-1}\left(\frac{1}{\mathrm{i}k}\frac{\mathrm{d}}{\mathrm{d}r} - \frac{1}{r}M_{zz}^{(1)}\right).$$

The waves characterized by η_1, ζ_1 and η_2, ζ_2 correspond to two independent solutions of equations (4) which are expressed by Bessel functions of the first and second kind, respectively. There are other solutions of equation (8), e.g. modified Bessel functions I_ν and K_ν, as well as Hankel functions of the first $H_\nu^{(1)}$ and second $H_\nu^{(2)}$ kind. Hankel function of the first (second) kind $H_\nu^{(1,2)}(r) = J_\nu(r) \pm \mathrm{i}Y_\nu(r)$ correspond to the divergent (converging) cylindrical wave. The quantities containing Hankel functions we will denote as letters with a tilde, for example $\tilde{\eta}$ and $\tilde{\zeta}$. Tensor notation for cylindrical waves is analogous to the notation for forward and backward plane waves.

Tensors η and ζ are very useful for describing multilayer systems because they determine field components that are continuous at cylindrical interfaces. Using these tensors we can define another two quantities: the transfer matrix (characteristic matrix, evolution operator)

$$\Omega_a^r = \begin{pmatrix} \eta_1(r) & \eta_2(r) \\ \zeta_1(r) & \zeta_2(r) \end{pmatrix}\begin{pmatrix} \eta_1(a) & \eta_2(a) \\ \zeta_1(a) & \zeta_2(a) \end{pmatrix}^{-1} \tag{12}$$

and the impedance tensor

$$\Gamma_m = \zeta_m\eta_m^{-1} \qquad m = 1, 2. \tag{13}$$

The transfer matrix Ω_a^r allows us to find the tangential field components in any point r if the initial vector $\boldsymbol{W}(a)$ is known: $\mathbf{W}(r) = \Omega_a^r\mathbf{W}(a)$. So, the quantity Ω_a^r expresses the spatial evolution of an electromagnetic field. The impedance tensor is the general linear relationship between electric and magnetic fields for each eigenwave: $\boldsymbol{E}_{tm} = \Gamma_m\boldsymbol{H}_{tm}$. We can apply inverse matrices (in equations (12) and (13)), if η and ζ are presented as two-dimensional matrices. If η and ζ are three-dimensional matrices, then we should use pseudoinversion instead of inversion.

Total field components can be computed by means of matrix V:

$$\begin{pmatrix} \boldsymbol{H}(\boldsymbol{r}) \\ \boldsymbol{E}(\boldsymbol{r}) \end{pmatrix} = \mathrm{e}^{\mathrm{i}\beta z + \mathrm{i}\nu\varphi}V(r)\boldsymbol{W}(r) \qquad V = \begin{pmatrix} I_r + \boldsymbol{e}_r \otimes \boldsymbol{v}_1 & \boldsymbol{e}_r \otimes \boldsymbol{v}_2 \\ \boldsymbol{e}_r \otimes \boldsymbol{v}_3 & I_r + \boldsymbol{e}_r \otimes \boldsymbol{v}_4 \end{pmatrix}. \tag{14}$$

An example of application of the formulae is presented below. For isotropic media with dielectric permittivity ε and magnetic permeability μ one obtains

$$\begin{aligned} \eta_1 &= J_\nu(qr)\left(\boldsymbol{e}_z - \frac{\beta\nu}{q^2 r}\boldsymbol{e}_\varphi\right) \otimes \boldsymbol{e}_z + \frac{\mathrm{i}k\varepsilon}{q}J_\nu'(qr)\boldsymbol{e}_\varphi \otimes \boldsymbol{e}_\varphi \\ \zeta_1 &= -\frac{\mathrm{i}k\mu}{q}J_\nu'(qr)\boldsymbol{e}_\varphi \otimes \boldsymbol{e}_z + J_\nu(qr)\left(\boldsymbol{e}_z - \frac{\beta\nu}{q^2 r}\boldsymbol{e}_\varphi\right) \otimes \boldsymbol{e}_\varphi \end{aligned} \tag{15}$$

where $q = \sqrt{k^2\varepsilon\mu - \beta^2}$, $J_\nu'(x) = \mathrm{d}J_\nu(x)/\mathrm{d}x$.

3. Light scattering by multilayer cylinders

Let the electromagnetic wave, the field strengths of which are $\boldsymbol{H}^{(0)}$ and $\boldsymbol{E}^{(0)}$, be incident from a vacuum ($\varepsilon = 1$, $\mu = 1$) on the n-layered cylindrical particle with bianisotropic constitutive parameters

$$(\varepsilon, \mu, \alpha, \kappa) = \begin{cases} (\varepsilon^{(1)}, \mu^{(1)}, \alpha^{(1)}, \kappa^{(1)}) & \text{for } 0 < r < a_1 \\ (\varepsilon^{(j)}, \mu^{(j)}, \alpha^{(j)}, \kappa^{(j)}) & \text{for } a_{j-1} < r < a_j, \qquad j = 2, \ldots, n. \end{cases} \tag{16}$$

We assume that the longitudinal length of the cylindrical particle is much greater than the wavelength. Therefore, an infinite length for the particle can be considered.

The incident wave induces the field inside the cylinder. The values of the field strengths in the outer nth cladding can be written as

$$\begin{pmatrix} \boldsymbol{H}(r, \varphi, z) \\ \boldsymbol{E}(r, \varphi, z) \end{pmatrix} = \int_{-\infty}^{\infty} \sum_{\nu=-\infty}^{\infty} \mathrm{e}^{\mathrm{i}\beta z + \mathrm{i}\nu\varphi} V(r) \Omega_{a_1}^{r}[\nu] \begin{pmatrix} I_r \\ \Gamma_\nu \end{pmatrix} \boldsymbol{b}_\nu(\beta)\, \mathrm{d}\beta \tag{17}$$

where $\boldsymbol{b}_\nu(\beta)$ are vector field amplitudes, $\Omega_{a_1}^{r}[\nu]$ is the evolution operator for the νth cylindrical wave and $\Gamma_\nu = \Gamma_\nu(a_1)$ is the wave impedance tensor at the interface $r = a_1$ in the first layer.

The scattered wave propagates in a vacuum and is described as follows:

$$\begin{pmatrix} \boldsymbol{H}^{(\mathrm{sc})}(r, \varphi, z) \\ \boldsymbol{E}^{(\mathrm{sc})}(r, \varphi, z) \end{pmatrix} = \int_{-\infty}^{\infty} \sum_{\nu=-\infty}^{\infty} \mathrm{e}^{\mathrm{i}\beta z + \mathrm{i}\nu\varphi} V^{(\mathrm{sc})}(r) \begin{pmatrix} I_r \\ \tilde{\Gamma}_\nu(r) \end{pmatrix} \tilde{\eta}_{1\nu}(r) \tilde{\eta}_{1\nu}^{-1}(a_n) \boldsymbol{b}_\nu^{(\mathrm{sc})}(\beta)\, \mathrm{d}\beta. \tag{18}$$

The quantities with tildes are expressed in terms of the Hankel function of the first kind $H_\nu^{(1)}$. During scattering we are interested in the fields $\boldsymbol{H}^{(\mathrm{sc})}$, $\boldsymbol{E}^{(\mathrm{sc})}$ in infinity. At $r \to \infty$ the Hankel function corresponds to the divergent cylindrical wave $H_\nu^{(1)}(qr) \approx C\mathrm{e}^{\mathrm{i}qr}/\sqrt{r}$, where $C = \text{const}$. Replacing ε, μ, J_ν in (15) by $\varepsilon = 1$, $\mu = 1$, $H_\nu^{(1)}$, respectively, we obtain at the limit $r \to \infty$

$$\begin{aligned} &\tilde{\eta}_{1\nu}(r) \approx C \frac{\mathrm{e}^{\mathrm{i}qr}}{\sqrt{qr}} \left(\boldsymbol{e}_z \otimes \boldsymbol{e}_z - \frac{k}{q} \boldsymbol{e}_\varphi \otimes \boldsymbol{e}_\varphi \right) \qquad \tilde{\zeta}_{1\nu}(r) \approx C \frac{\mathrm{e}^{\mathrm{i}qr}}{\sqrt{qr}} \left(\boldsymbol{e}_z \otimes \boldsymbol{e}_\varphi + \frac{k}{q} \boldsymbol{e}_\varphi \otimes \boldsymbol{e}_z \right) \\ &\tilde{\Gamma}_\nu(r) \approx \frac{k}{q} \boldsymbol{e}_\varphi \otimes \boldsymbol{e}_z - \frac{q}{k} \boldsymbol{e}_z \otimes \boldsymbol{e}_\varphi \equiv \tilde{\Gamma} \qquad V_l^{(\mathrm{sc})}(r) \approx E \equiv \begin{pmatrix} I_r & 0 \\ 0 & I_r \end{pmatrix}. \end{aligned} \tag{19}$$

The impedance tensor depends neither on azimuthal number ν nor radial coordinate r. Therefore, the scattered field can be rewritten as

$$\begin{pmatrix} \boldsymbol{H}^{(\mathrm{sc})}(r, \varphi, z) \\ \boldsymbol{E}^{(\mathrm{sc})}(r, \varphi, z) \end{pmatrix} = \int_{-\infty}^{\infty} \frac{\mathrm{e}^{\mathrm{i}qr}}{\sqrt{r}} \left(\frac{\mathrm{e}^{\mathrm{i}qa_n}}{\sqrt{a_n}} \right)^{-1} \begin{pmatrix} I_r \\ \tilde{\Gamma} \end{pmatrix} \sum_{\nu=-\infty}^{\infty} \mathrm{e}^{\mathrm{i}\beta z + \mathrm{i}\nu\varphi} \boldsymbol{b}_\nu^{(\mathrm{sc})}(\beta)\, \mathrm{d}\beta. \tag{20}$$

Unknown amplitudes $\boldsymbol{b}_\nu(\beta)$ and $\boldsymbol{b}_\nu^{(\mathrm{sc})}(\beta)$ can be determined from continuity conditions for the tangential components of electric and magnetic fields at the outer surface $r = a_n$ of the multilayer cylinder:

$$\begin{pmatrix} \boldsymbol{H}_t^{(0)}(a_n, \varphi, z) \\ \boldsymbol{E}_t^{(0)}(a_n, \varphi, z) \end{pmatrix} + \begin{pmatrix} \boldsymbol{H}_t^{(\mathrm{sc})}(a_n, \varphi, z) \\ \boldsymbol{E}_t^{(\mathrm{sc})}(a_n, \varphi, z) \end{pmatrix} = \begin{pmatrix} \boldsymbol{H}_t(a_n, \varphi, z) \\ \boldsymbol{E}_t(a_n, \varphi, z) \end{pmatrix}. \tag{21}$$

For an infinitely long cylinder the longitudinal coordinate z takes values from $-\infty$ to $+\infty$.

By substituting equations (17), (20) and designating $\boldsymbol{W}^{(0)} = (\boldsymbol{H}_t^{(0)}, \boldsymbol{E}_t^{(0)})^{\mathrm{T}}$ we express the boundary conditions as follows

$$\begin{aligned} \boldsymbol{W}^{(0)}(a_n, \varphi, z) &+ \int_{-\infty}^{\infty} \begin{pmatrix} I_r \\ \tilde{\Gamma} \end{pmatrix} \sum_{\nu=-\infty}^{\infty} \mathrm{e}^{\mathrm{i}\beta z + \mathrm{i}\nu\varphi} \boldsymbol{b}_\nu^{(\mathrm{sc})}(\beta) \mathrm{d}\beta \\ &= \int_{-\infty}^{\infty} \sum_{\nu=-\infty}^{\infty} \mathrm{e}^{\mathrm{i}\beta z + \mathrm{i}\nu\varphi} \Omega_{a_1}^{a_n}[\nu] \begin{pmatrix} I_r \\ \Gamma_\nu \end{pmatrix} \boldsymbol{b}_\nu(\beta) \mathrm{d}\beta. \end{aligned} \tag{22}$$

Multiplying equation (22) by $\mathrm{e}^{-\mathrm{i}\beta' z-\mathrm{i}\nu'\varphi}/(2\pi)^2$ and integrating over z from $-\infty$ to ∞ and over φ from 0 to 2π we obtain

$$\boldsymbol{W}_\nu^{(0)}(a_n,\beta)+\begin{pmatrix} I_r \\ \tilde{\Gamma}\end{pmatrix}\boldsymbol{b}_\nu^{(\mathrm{sc})}(\beta)=\Omega_{a_1}^{a_n}[\nu]\begin{pmatrix} I_r \\ \Gamma_\nu\end{pmatrix}\boldsymbol{b}_\nu(\beta) \tag{23}$$

where

$$\boldsymbol{W}_\nu^{(0)}(a_n,\beta)=\frac{1}{(2\pi)^2}\int_{-\infty}^{\infty}\mathrm{d}z\,\mathrm{e}^{-\mathrm{i}\beta z}\int_0^{2\pi}\mathrm{d}\varphi\,\mathrm{e}^{-\mathrm{i}\nu\varphi}\boldsymbol{W}^{(0)}(a_n,\varphi,z). \tag{24}$$

Amplitudes of the scattered field can be easily found from (23) if we multiply this equation by block matrix $(\Gamma_\nu - I_r)\Omega_{a_n}^{a_1}[\nu]$:

$$\boldsymbol{b}_\nu^{(\mathrm{sc})}(\beta)=-\left[(\Gamma_\nu - I_r)\Omega_{a_n}^{a_1}[\nu]\begin{pmatrix} I_r \\ \tilde{\Gamma}\end{pmatrix}\right]^{-1}(\Gamma_\nu - I_r)\Omega_{a_n}^{a_1}[\nu]\boldsymbol{W}_\nu^{(0)}(a_n,\beta) \tag{25}$$

where $\Omega_{a_n}^{a_1}=(\Omega_{a_1}^{a_n})^{-1}$.

The scattered field can be characterized by the differential scattering cross-section (the power radiated in the direction $\boldsymbol{e}_r$ per unit solid angle)

$$\frac{\mathrm{d}\sigma}{\mathrm{d}o}=r\frac{|\boldsymbol{H}^{(\mathrm{sc})}|^2}{|\boldsymbol{H}^{(0)}|^2}. \tag{26}$$

By substituting the expression for the scattered magnetic field (20) into the formula for the differential cross-section one obtains

$$\frac{\mathrm{d}\sigma}{\mathrm{d}o}(\varphi,z)=\frac{a_n}{|\boldsymbol{H}^{(0)}|^2}\left|\int_{-\infty}^{\infty}\sum_{\nu=-\infty}^{\infty}\mathrm{e}^{\mathrm{i}\beta z+\mathrm{i}\nu\varphi}\boldsymbol{b}_\nu^{(\mathrm{sc})}(\beta)\mathrm{d}\beta\right|^2. \tag{27}$$

Angle φ averaging results in

$$\frac{\mathrm{d}\sigma}{\mathrm{d}z}(z)=\frac{a_n}{|\boldsymbol{H}^{(0)}|^2}\sum_{\nu=-\infty}^{\infty}\left|\int_{-\infty}^{\infty}\mathrm{e}^{\mathrm{i}\beta z}\boldsymbol{b}_\nu^{(\mathrm{sc})}(\beta)\mathrm{d}\beta\right|^2. \tag{28}$$

The scattering angle θ can be easily introduced as follows: $z=\cot\theta$. Therefore, equation (28) can be rewritten as

$$\frac{\mathrm{d}\sigma}{\mathrm{d}\theta}(\theta)=\frac{a_n}{\sin^2\theta|\boldsymbol{H}^{(0)}|^2}\sum_{\nu=-\infty}^{\infty}\left|\int_{-\infty}^{\infty}\mathrm{e}^{\mathrm{i}\beta\cot\theta}\boldsymbol{b}_\nu^{(\mathrm{sc})}(\beta)\mathrm{d}\beta\right|^2. \tag{29}$$

4. Example and conclusion

Let us consider a y-polarized Gaussian beam

$$\boldsymbol{H}^{(0)}=\exp(\mathrm{i}kz\cos\theta_0+\mathrm{i}kx\sin\theta_0)\exp\left(-\frac{(x\cos\theta_0-z\sin\theta_0)^2}{2w^2}\right)\boldsymbol{e}_y$$

incident onto the two-layer cylinder with bianisotropic core ($\varepsilon^{(1)}=\varepsilon_1 I_z+\varepsilon_2\boldsymbol{e}_z\otimes\boldsymbol{e}_z$, $\mu^{(1)}=\mu_1 I_z+\mu_2\boldsymbol{e}_z\otimes\boldsymbol{e}_z$, $\alpha=\kappa=\mathrm{i}\chi\boldsymbol{e}_z^{\times}$) and isotropic cladding ($\varepsilon^{(2)}=\varepsilon$, $\mu^{(2)}=\mu$, $\alpha=\kappa=0$), where θ_0 is the angle of incidence and w is the beam waist (see figure 1). In cylindrical coordinates tangential components of the incident electromagnetic field take the form

$$\boldsymbol{H}_t^{(0)}=F(r,\varphi,z)\cos\varphi\boldsymbol{e}_\varphi \qquad \boldsymbol{E}_t^{(0)}=\mathrm{i}F(r,\varphi,z)\left[\left(\mathrm{i}\sin\theta_0-\frac{\cos\theta_0}{kw^2}(x\cos\theta_0-z\sin\theta_0)\right)\boldsymbol{e}_z\right.$$
$$\left.+\sin\varphi\left(\mathrm{i}\cos\theta_0+\frac{\sin\theta_0}{kw^2}(x\cos\theta_0-z\sin\theta_0)\right)\boldsymbol{e}_\varphi\right] \tag{30}$$
$$F(r,\varphi,z)=\exp(\mathrm{i}kz\cos\theta_0+\mathrm{i}kr\cos\varphi\sin\theta_0)\exp\left(-\frac{(r\cos\varphi\cos\theta_0-z\sin\theta_0)^2}{2w^2}\right).$$

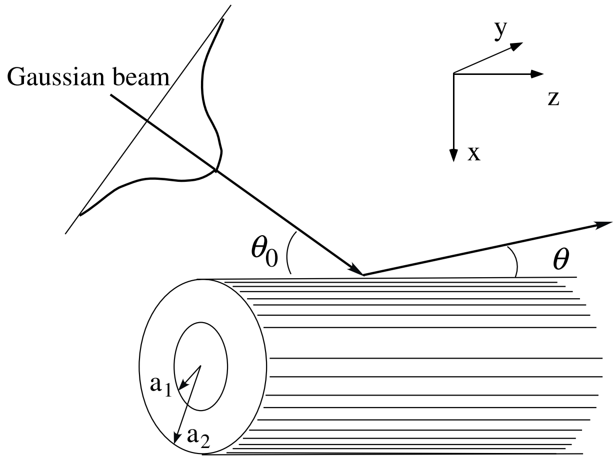

Figure 1. Gaussian beam scattering by a two-layer bianisotropic cylinder.

The differential cross-section can be easily found if the following steps are taken: (i) calculate vectors $\boldsymbol{W}_\nu^{(0)}(a_n, \beta)$ applying formula (24); (ii) compute scattering field amplitudes $\boldsymbol{b}_\nu^{(\mathrm{sc})}(\beta)$ using equation (25); (iii) substitute the scattering field amplitudes found above into equation (29). In denominator of (29) we shall take $|\boldsymbol{H}^{(0)}(x = 0, z = 0)|^2 = 1$. For calculation of integrals we can use fast Fourier transform.

To determine the amplitudes $\boldsymbol{b}_\nu^{(\mathrm{sc})}(\beta)$ we should use the impedance tensor $\tilde{\Gamma}$ (see equation (19)), as well as the evolution operator (12) for an isotropic medium and the impedance tensor (13) for a bianisotropic medium, which can be expressed by means of auxiliary tensors η and ζ. These tensors have already been written for an isotropic medium as equation (15). For a bianisotropic medium the tensors η and ζ are equal to (see papers [25, 26])

$$\begin{aligned} \eta_1 &= J_\nu(q_1 r)\left(\boldsymbol{e}_z - \frac{\mu_2 \nu(\beta - \mathrm{i}k\chi)}{\mu_1 q_1^2 r}\boldsymbol{e}_\varphi\right) \otimes \boldsymbol{e}_z + \frac{\mathrm{i}k\varepsilon_2 J_\nu'(q_2 r)}{q_2}\boldsymbol{e}_\varphi \otimes \boldsymbol{e}_\varphi, \\ \zeta_1 &= -\frac{\mathrm{i}k\mu_2 J_\nu'(q_1 r)}{q_1}\boldsymbol{e}_\varphi \otimes \boldsymbol{e}_z + J_\nu(q_2 r)\left(\boldsymbol{e}_z - \frac{\varepsilon_1 \nu(\beta + \mathrm{i}k\chi)}{\varepsilon_1 q_2^2 r}\boldsymbol{e}_\varphi\right) \otimes \boldsymbol{e}_\varphi, \end{aligned} \tag{31}$$

where $q_1^2 = k^2\varepsilon_1\mu_2 - (k^2\chi^2 + \beta^2)\mu_2/\mu_1$, $q_2^2 = k^2\varepsilon_2\mu_1 - (k^2\chi^2 + \beta^2)\varepsilon_2/\varepsilon_1$.

Differential cross-sections can be computed for each ν; they are called partial cross-sections. In figure 2 we present partial differential cross-sections for $\nu = -6, \ldots, 6$. The total differential cross-section is the sum of all partial cross-sections. In real calculations the sum of a finite number of partial differential cross-sections is used (the sum from -6 to 6 in figure 2). The dependence of partial differential cross-sections on scattering angle has the same behaviour for all ν. The greatest contribution to $\mathrm{d}\sigma/\mathrm{d}o$ is for $\nu = \pm 1$, due to the presence of $\cos\varphi$ and $\sin\varphi$ in the initial fields. Total differential cross-section almost repeat the shape of the curve for $|\nu| = 1$. Partial cross-sections from $|\nu| = 1$ to 6 follow one after another. The case $\nu = 0$ is out of this sequence. The contributions for $|\nu| > 6$ are much smaller than that for $|\nu| = 1$ and can therefore be neglected. Great scattering for small scattering angles is due to the guiding properties of the cylinder, which localizes the energy near its interface.

In figure 3 the θ_0-dependence of differential cross-sections is presented. For small angles of incidence the partial contribution of $\nu = \pm 1$ dominates. For large angles (close to 90°) differential cross-sections for higher order νs play an important part. The total differential

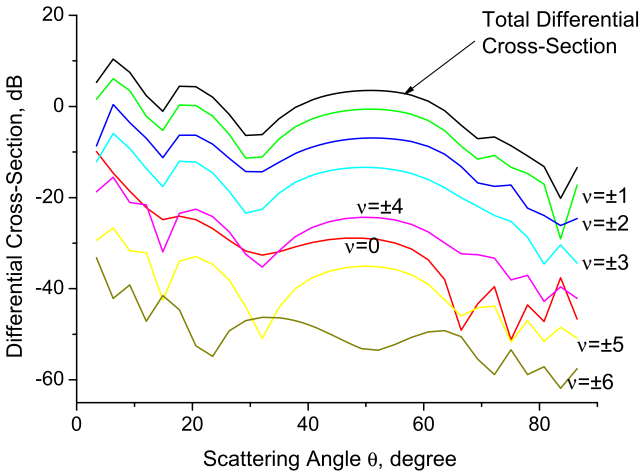

Figure 2. Partial and total differential cross-sections versus scattering angle. Parameters: $\varepsilon_1 = 2.1$, $\mu_1 = 1.25$, $\varepsilon_2 = 2$, $\mu_2 = 1.2$, $\chi = 0.1$, $\varepsilon = 2.5$, $\mu = 1$, $ka_1 = 2$, $ka_2 = 3$, $kw = 2$, $\theta_0 = 30°$.

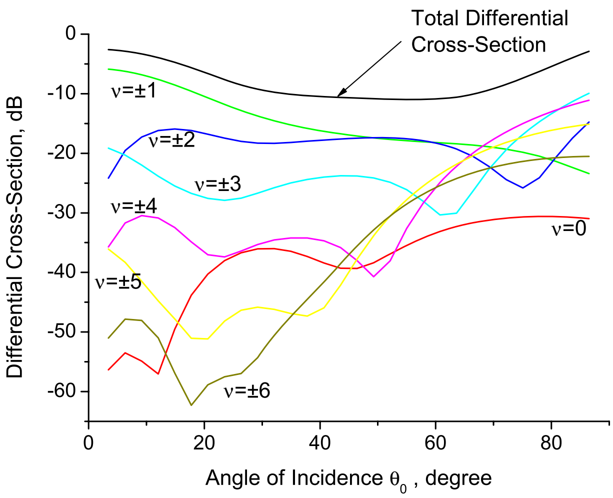

Figure 3. Partial and total differential cross-sections versus angle of incidence. Parameters: $\varepsilon_1 = 2.1$, $\mu_1 = 1.25$, $\varepsilon_2 = 2$, $\mu_2 = 1.2$, $\chi = 0.1$, $\varepsilon = 2.5$, $\mu = 1$, $ka_1 = 2$, $ka_2 = 3$, $kw = 2$, scattering angle $\theta = 60°$.

cross-section takes maximal values for small and large differential cross-sections (see figure 4). For angles of incidence close to 90° the scattering depends on scattering angle mainly as $1/\sin^2\theta$, because the value $10\lg(\sin 60°/\sin 20°)^2 \approx 8$ dB is the gap between the curves for $\theta = 60°$ and 20°.

Since we are considering a bianisotropic cylinder, it is interesting to trace the dependence on the bianisotropic medium parameter χ. In figure 5 one can see that the dependence on χ is weak. Usually, the parameter χ is much smaller than the dielectric permittivity. However, even if we take large values ($\chi = 0.3$), a small increase (0.03 dB) is observed. Such a weak dependence can be used for accurate control of the cross-section.

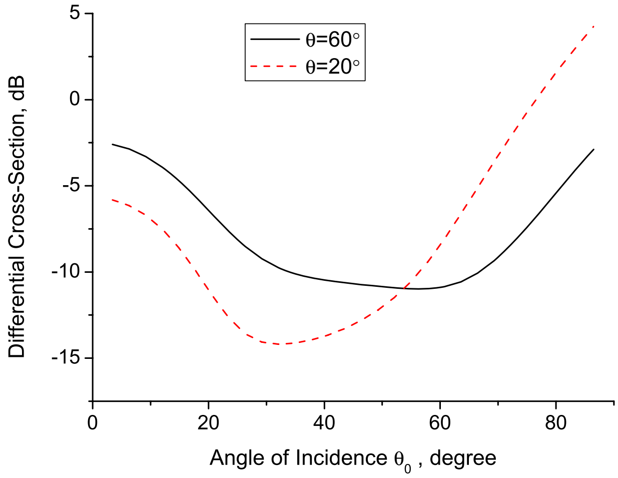

Figure 4. Total differential cross-sections versus angle of incidence for two values of scattering angle $\theta = 60°$ and $20°$. Parameters: $\varepsilon_1 = 2.1$, $\mu_1 = 1.25$, $\varepsilon_2 = 2$, $\mu_2 = 1.2$, $\chi = 0.1$, $\varepsilon = 2.5$, $\mu = 1$, $ka_1 = 2$, $ka_2 = 3$, $kw = 2$.

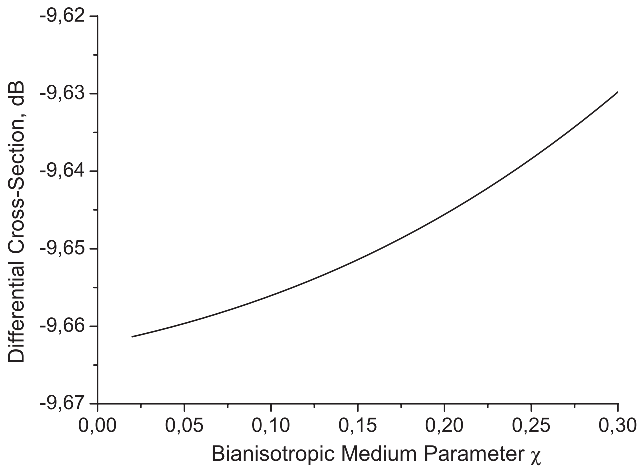

Figure 5. Differential cross-section versus bianisotropic medium parameter χ. Parameters: $\varepsilon_1 = 2.1$, $\mu_1 = 1.25$, $\varepsilon_2 = 2$, $\mu_2 = 1.2$, $\varepsilon = 2.5$, $\mu = 1$, $ka_1 = 2$, $ka_2 = 3$, $kw = 2$, $\theta = 30°$, $\theta_0 = 45°$.

In figure 6 the differential cross-section depending on the Gaussian beam waist is presented. For small waists the differential cross-section increases due to the increase in the incident beam energy. The energy $\int_{\infty}^{\infty} |\boldsymbol{E}^{(0)}| \mathrm{d}x_1$ behaves like $1/w$ for small w and goes to infinity, when $w \longrightarrow 0$, where x_1 is the coordinate orthogonal to the beam incidence direction. For large waists the total differential cross-section arises again, because in this case the beam energy depends linearly on w.

There is no strong dependence on the cylinder core radius, because the refractive indices of the bianisotropic core and isotropic cladding are close. In figure 7 the core radius is fixed, while the radius of the cladding a_2 is the variable. There are regions of cladding radius for which one or another partial differential cross-section is considerable. For example, for $\nu = 3$

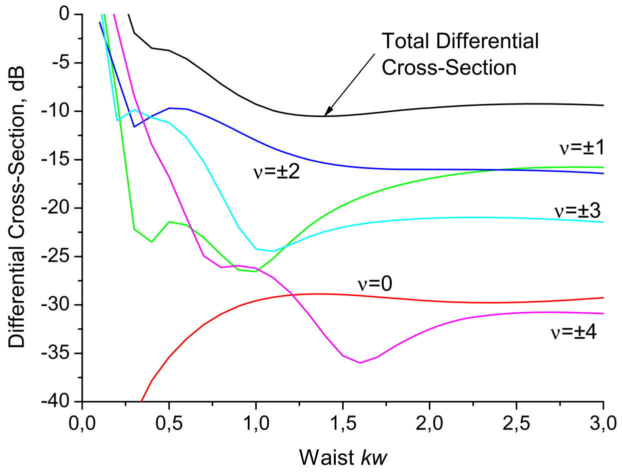

Figure 6. Partial and total differential cross-sections versus Gaussian beam waist. Parameters: $\varepsilon_1 = 2.1$, $\mu_1 = 1.25$, $\varepsilon_2 = 2$, $\mu_2 = 1.2$, $\chi = 0.1$, $\varepsilon = 2.5$, $\mu = 1$, $ka_1 = 2$, $ka_2 = 3$, $\theta = 30°$, $\theta_0 = 45°$.

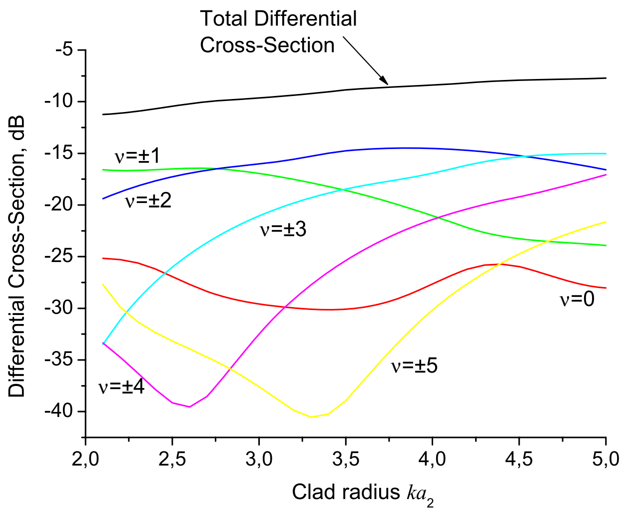

Figure 7. Partial and total differential cross-sections versus cladding radius. Parameters: $\varepsilon_1 = 2.1$, $\mu_1 = 1.25$, $\varepsilon_2 = 2$, $\mu_2 = 1.2$, $\chi = 0.1$, $\varepsilon = 2.5$, $\mu = 1$, $ka_1 = 2$, $kw = 2$, $\theta = 30°$, $\theta_0 = 45°$.

this region starts with the value $ka_2 \approx 4$. Since for a greater cladding radius more beam energy is scattered, the total differential cross-section increases.

In conclusion, we have developed an effective matrix method for describing light scattering by bianisotropic cylindrical particles. The main advantages of the approach are the possibility to apply it to multilayer cylinders, the possibility to consider an arbitrary beam and the possibility to easily write the algorithm for computations. Complicated mathematics is necessary to solve the scattering problem in a sufficiently general case. However, using the final formulae we can now numerically calculate the scattering characteristics. The example of the scattering of a Gaussian beam confirms the functionality of the method.

Acknowledgment

The work was supported by the Basic Research Foundation of Belarus, grant F05MS-028.

References

[1] Newton R G 1982 *Scattering Theory of Waves and Particles* (Heidelberg: Springer)
[2] Bohren C F and Huffman D R 1983 *Absorption and Scattering of Light by Small Particles* (New York: Wiley)
[3] Snyder A W and Love J D 1983 *Optical Waveguide Theory* (New York: Chapman and Hall)
[4] Wolinski T R 2000 Polarimetric optical fibres and sensors *Progress in Optics* vol XL ed E Wolf (Amsterdam: Elsevier) pp 1–70
[5] Yariv A and Winsor H V 1980 Proposal for detection of magnetic fields through magnetostrictive perturbation of optical fibres *Opt. Lett.* **5** 87–9
[6] Wolinski T R and Bock W J 1993 Simultaneous twist and pressure effects in highly birefringent single-mode bow-tie fibres *J. Lightwave Technol.* **11** 389–94
[7] Limeres J, Calvo M L, Enoch J M and Lakshminarayanan V 2003 Light scattering by an array of birefringent optical waveguides: theoretical foundations *J. Opt. Soc. Am.* B **20** 1542–9
[8] Bohren C F 1978 Scattering of electromagnetic waves by an optically active cylinder *J. Colloid Interface Sci.* **66** 105–9
[9] Kluskens S and Newman H 1990 Scattering by a chiral cylinder of arbitrary cross section *IEEE Trans. Antennas Propag.* **38** 1448–55
[10] Al-Kanhal M A and Arvas E 1996 Electromagnetic scattering from a chiral cylinder of arbitrary cross-section *IEEE Trans. Antennas Propag.* **44** 1041–8
[11] Kuzmiak V and Maradudin A A 2002 Scattering properties of a cylinder fabricated from a left-handed material *Phys. Rev.* B **66** 045116
[12] Ruppin R 2004 Surface polaritons and extinction properties of a left-handed material cylinder *J. Phys.: Condens. Matter* **16** 5991–8
[13] Li C and Shen Z 2003 Electromagnetic scattering by a conducting cylinder coated with metamaterials *Prog. Electromag. Res.* **42** 91–105
[14] Veselago V G 1968 The electrodynamics of substances with simultaneously negative values of ε and μ *Sov. Phys.—Usp.* **10** 509–14
[15] Smith D R *et al* 2000 Composite medium with simultaneously negative permeability and permittivity *Phys. Rev. Lett.* **84** 4184–7
[16] Mignon H *et al* 1996 Measurements of cylindrical particles using phase Doppler anemometry *Appl. Opt.* **25** 5180–90
[17] Gauchet N *et al* 1997 Application of generalised Lorenz–Mie theory for cylinders to cylindrical particle characterization by phase-Doppler anemometry *Opt. Diagn. Eng.* **2** 1–6
[18] Konistis K and Tsalamengas J L 1997 Plane wave scattering by an array of bianisotropic cylinders enclosed by another one in an unbounded bianisotropic scace: Oblique incidence *J. Electromag. Waves Appl.* **11** 1073–90
[19] Tsalamengas J L 1998 Diffraction by a strip in an unbounded gyrotropic or biisotropic medium *IEEE Trans. Antennas Propag.* **46** 1065–73
[20] Tsalamengas J L 2005 Diffraction of obliquely incident waves by a strip in a bianisotropic medium *IEEE Trans. Antennas Propag.* **53** 260–9
[21] Al Sharkawy M, Elsherbeni A Z and Mahmoud S F 2004 Electromagnetic scattering from parallel chiral cylinders of circular crosssections using an iterative procedure *Prog. Electromag. Res.* **47** 87–110
[22] Yin W-Y and Li L-W 1999 Multiple scattering from gyrotropic bianisotropic cylinders of arbitrary cross sections using the modeling technique *Phys. Rev.* E **60** 918–25
[23] Zhang M, Yeo T S, Li L W and Leong M S 2003 Electromagnetic scattering by a multilayer gyrotropic bianisotropic circular cylinder *Prog. Electromag. Res.* **40** 91–111
[24] Sharma S K and Somerford D J 1999 Scattering of light in the eikonal approximation *Progress in Optics* vol XXXIX ed E Wolf (Amsterdam: Elsevier) pp 213–90
[25] Novitsky A V and Barkovsky L M 2005 Operator matrices for describing guiding propagation in circular bianisotropic fibres *J. Phys. A: Math. Gen.* **38** 391–404
[26] Novitsky A V and Barkovsky L M 2006 Spatial evolution of cylindrical beams in complex media *J. Phys. A: Math. Gen.* **39** 1521–36
[27] Novitsky A V and Barkovsky L M 2006 Evolution and impedance operators of spherically symmetric bianisotropic media *J. Phys. A: Math. Gen.* **39** 7543–60
[28] Fedorov F I 1976 *Theory of Gyrotropy* (Minsk: Nauka i Tehnika)
[29] Barkovskii L M, Borzdov G N and Lavrinenko A V 1987 Fresnel's reflection and transmission operators for stratified gyroanisotropic media *J. Phys. A: Math. Gen.* **20** 1095–106